Cancer Immunol Immunother (2013) 62:183–190
DOI 10.1007/s00262-012-1318-1

ORIGINAL ARTICLE

A knockdown of Maml1 that results in melanoma cell senescence promotes an innate and adaptive immune response

Shijun Kang · Jianmin Xie · Jingxia Miao · Rong Li · Wangjun Liao · Rongcheng Luo

Received: 4 December 2011 / Accepted: 6 July 2012 / Published online: 5 August 2012

Abstract Maml1 is emerging as a coactivator of many signaling pathways, including the Notch and Wnt pathways. Targeting Maml1 in melanoma cells efficiently knocks down the downstream transcriptional repressors Hey1 and Hes1, resulting in melanoma cell senescence, cellular differentiation, and increased melanin production. Significantly, higher IFNβ and chemokine gene transcripts have been observed, together with increased STAT1 and decreased STAT3 and NF-κB signaling activities. Although decreased cell proliferation contributes to slower tumor growth in vivo, the depletion of NK and $CD8^+$ T cells in an *shMaml1-B16* tumor carrier mouse leads to more rapid tumor growth than that observed in control *shC002-B16* tumors. This result demonstrates that the knockdown of Maml1 transcription and function contributes to increased immune surveillance. The knockdown of *Maml1* transcription in the human melanoma cell line M537 also results in senescence, IFNβ upregulation, increased chemokine gene expression, and greater NK and $CD8^+$ T cell migration in a transwell system. This study demonstrated that targeting *Maml1*-induced tumor cell senescence and differentiation may alter the tumor microenvironment and cytokine and chemokine profiles and may also promote innate and adaptive immune cell infiltration and function.

Keywords *shMaml1* · Cellular senescence · Innate and adaptive immune cells · IFNβ and chemokines

S. Kang · J. Xie · J. Miao · R. Li · W. Liao · R. Luo (✉)
Department of Oncology, Nanfang Hospital, Southern Medical University, Guangzhou, China
e-mail: luorcluo@yahoo.com

S. Kang
e-mail: drkang6@163.com

Abbreviations

Maml1	Mastermind-like protein-1
siMaml1	*Small interfering Maml1* RNA
Hes1	Hairy/enhancer-of-split 1
Hey1	Hairy/enhancer-of-split related with YRPW motif 1
CCL2	MCP-1, monocyte chemoattractant-1
CCL3	Macrophage inflammatory protein-1α (MIP-1α)
CCL5	Regulated upon activation normal T cell expressed and secreted (RANTES)
CCL18	Macrophage inflammatory protein-4 (MIP-4, PARC)
CXCL9	Monokine induced by gamma interferon (Mig)
CXCL10	Interferon gamma-induced protein-10 (IP-10)
CXCL11	Interferon-inducible T cell alpha chemoattractant (I-TAC, IP-9)

Introduction

The developmental proteins such as Notch, Wnt, and Hedgehog are key regulators of cell fate, proliferation, and differentiation. Their signaling pathways are related and are frequently activated in neoplasms from cancer stem cells that are capable of self-renewal, which often leads to the development of tumor resistance to therapy, tumor recurrence, and metastasis [1–4]. The Notch receptor proteins are highly expressed in melanoma cells and are constitutively cleaved to release the intracellular domain (NICD). Mastermind-like protein-1 (Maml1) directly binds to the most conserved ankyrin repeat domain of the four Notch receptors (NICD1–4), and Maml1 also interacts with

CSL to form a stable DNA-binding ternary complex, thereby leading to the transcriptional activation of Hes1 and Hey1 [4–8]. A recent study discovered that Maml1 also participates in the Wnt/β-catenin signaling pathway independently of the Notch signaling pathway. Maml1 is recruited by β-catenin to the cyclin D1 and c-Myc promoters to activate tumor cell survival [9]. In neural precursor cells, Maml1, β-catenin, and NICD form a complex within the promoter region of the *Hes1* gene, inducing its expression and simultaneously promoting cellular proliferation and inhibiting differentiation [10]. These studies support a new role for Maml1 as an essential component of Notch and Wnt/β-catenin signaling-mediated tumorigenesis and suggest that Maml1 could be an alternative target for both the Notch and Wnt/β-catenin signaling pathways.

Hes1 encodes a basic helix-loop-helix transcription factor that functions as a classical effector of the Notch signaling pathway [4–8]. However, recent reports indicated that, in stem-like cells, Hedgehog elicited a strong Hes1 response independent of canonical Notch signaling [11–14]. Elsewhere, Schreck's group found that targeting the Notch pathway using a g-secretase inhibitor increases Hedgehog activity, and the inhibition of both Notch and Hedgehog dramatically decreases the growth of glioblastoma and melanoma cell lines and low-passage neurospheres derived from primary human tumors [15]. The Hes1 signaling pathway is activated in several types of tumor cells. Activation of this signaling pathway allows these tumor cells to evade differentiation; therefore, irreversible senescence contributes to tumorigenesis [16, 17]. Maml1 is an essential coactivator that facilitates Notch-induced *Hes1* and *Hey1* transcription [7, 18]. Recent studies have indicated that Maml1 directly regulates NF-κB signaling and cell survival [19]. All of these data support our hypothesis that targeting Maml1 may regulate the Notch, Wnt, and Hedgehog signaling pathways simultaneously and may serve as a novel anticancer strategy by inhibiting cell proliferation and promoting cell differentiation and irreversible senescence [19–21].

Previously, we used *siMaml1* to inhibit the transcriptional activation of *Hes1/Hey1* in melanoma cells, leading to the upregulation of multiple cytokines, including CCL2 [7]. However, researchers found that due to the low siRNA concentrations caused by cell division and intracellular siRNA turnover, the duration of siRNA silencing is short [22]. To analyze the effects of Maml1 on cell differentiation and senescence, the *Maml1* gene must be silenced for a prolonged period of time. To accomplish this goal, we transfected several short-hairpin *Maml1* (*shMaml1*) lentiviral expression plasmids to achieve sustained gene silencing, and we established a stable *shMaml1*-transfected B16 melanoma cell line (*shMaml1-B16*). We found that there were only a fraction of *shMaml1-B16* cells undergoing apoptosis similar to the control plasmid *shC002-B16*-transfected cells or the parent B16 cells. However, we observed more *shMaml1-B16* cells with increased senescence-associated-β-galactosidase (SA-β-Gal) staining and increased cell differentiation based on increased melanin production. These cells secrete several immune-stimulating cytokines and chemokines in vitro. In syngeneic mice, *shMaml1-B16* cells formed tumors more slowly than control cells. Flow cytometry showed increased infiltration of immune cells, such as DC, NK, and $CD8^+$ T cells, in these tumors.

Materials and methods

Establishment of shMaml1-B16 and shC002-B16 cells

MISSION shRNA clones (clone ID sh138: TRCN0000115138 targeting NM_175334.2-1187s1c1; clone ID sh139: TRCN0000115139 targeting NM_175334.2-1019s1c1; clone ID sh140: TRCN0000115140 targeting NM_175334.2-2544s1c1; clone ID shmix: mixture of TRCN0000115138, TRCN0000115139, and TRCN0000115140; human clone ID sh353: TRCN0000003353 targeting NM_014757.x-585s1c1; and clone ID sh356: TRCN0000003356 targeting NM_014757.x-1907s1c1) are sequence-verified, lentiviral plasmids (pLKO.1-puro) purchased from Sigma-Aldrich. B16F10 cells were transfected, and stable *shMaml1-B16* cells were selected under optimized conditions using puromycin resistance (1 μg/ml) according the manufacturer's protocol. Briefly, the siGENOME SMARTpool (10 μl) was diluted in 90 μl of serum-free DMEM containing transfection reagents, incubated at room temperature for 15 min, and added to a 2×10^5 cells/ml cell culture at a range of concentrations. Transfections were conducted twice on consecutive days, and the cells were allowed to continue to grow for an additional 2 days at 37 °C in the presence of 5 % CO_2 before the puromycin selection. The nontarget, control lentiviral plasmid *shC002* validated the specific knockdown of *Maml1* by MISSION *shMaml1*.

Detection of SA-β-gal activity using confocal microscopy

SA-β-gal activity was measured at pH 6.0 for B16 cells and pH 5.5 for mouse tissue, as described previously. Briefly, the adherent cells were fixed with 0.5 % glutaraldehyde in PBS for 15 min, washed with PBS containing 1 mM $MgCl_2$, and stained for 5–6 h in PBS containing 1 mM $MgCl_2$, 1 mg/ml X-Gal (Roche, Indianapolis, IN, USA), 5 mM potassium ferricyanide, and 5 mM potassium ferrocyanide (Sigma-Aldrich, St. Louis, MO, USA). The

images were photographed at several magnifications using a Nikon camera.

Analysis of gene expression using RT-qPCR

The cells and tumors were homogenized in 1 ml Trizol (Invitrogen, Grand Island, NY, USA), and total RNA was precipitated from the aqueous phase using isopropyl alcohol after performing a chloroform separation. After DNase I treatment, cDNA was synthesized from 1 μg of total RNA using MLV-Reverse Transcriptase according to the manufacturer's directions. Real-time PCR (RT-qPCR) was performed using an ABI PRISM® 7300 Sequence Detection System with a Power SYBR Green PCR Master Mix (Applied Biosystems, Foster City, CA, USA). Changes in gene expression were calculated using comparative Ct values with β-actin as an endogenous gene control. The ΔCT was calculated, and the relative expression of each cytokine and chemokine was compared. Prevalidated primers and probes specific for *Maml1* (Mm00614627_m1), *Hey1* (Mm00468865_m1), *Hes1* (Mm01342805_m1), *CCL2* (Mm00441242_m1), *CCL5* (Mm01302427_m1), *CXCL9* (Mm00434946_m1), *CXCL10* (Mm00445235_m1), *CXCL11* (Mm00444662_m1), *CCL22* (Mm00436439_m1), and *β-actin* (Mm00525061_m1) were purchased from Applied Biosystems.

Immunoblotting and signaling inhibitors

Preparation of cytosolic extracts was carried out using a Nuclear Extract Kit (Active Motif, CA, USA) according to the manufacturer's recommendations. The concentrations of proteins in the nuclear and cytosolic fractions were measured using a microplate version of the Lowry assay (Micro BCA Protein Assay Reagent Kit, Pierce, IL, USA) with bovine serum albumin (BSA) standards. The lysates were separated using SDS-PAGE on a 10 % gel and then transferred to a nitrocellulose membrane. The membrane was blocked with blocking buffer (5 % nonfat dry milk in TBST (20 mM Tris–HCl, pH 7.5, and 0.5 % Tween 20)) for 1 h at room temperature and then incubated overnight with one of the following primary antibodies diluted in the blocking buffer: anti-phospho-STAT1, anti-phospho-STAT3, anti-phospho-IκBα (1:500; Cell Signaling Technologies, Beverly, MA, USA), rabbit anti-STAT1, anti-STAT3, anti-NFκB p65, or anti-β-actin (1:500; Santa Cruz Biotechnologies, Santa Cruz, CA, USA). An HRP-conjugated, anti-rabbit secondary antibody (Amersham, Arlington Heights, IL, USA) was used at a 1:10,000 dilution for 1 h at room temperature. The blots were visualized using an Amersham enhanced chemiluminescence (ECL) kit. A highly selective inhibitor of IκB kinase (BMS-345541), the STAT1 inhibitor fludarabine (Sigma-Aldrich, St. Louis, MO, USA), and the cell-permeable peptide STAT3 inhibitor LLL12 (BioVision, Mountain view, CA, USA) were applied to the cell cultures when necessary.

Tumor inoculation and tumor-infiltrating cell treatment and analysis

All mice were bred and maintained in a pathogen-free facility at the Medical Center. The mice were handled in accordance with the animal experimental guidelines set by the Institute of Animal Care and Use Committee (IACUC) for all experiments. C57BL/6 wild-type mice (6–7 weeks old) were purchased from the Laboratory Animal Center of Southern Medical University (Guangzhou, China). The mice were subcutaneously injected with *shMaml1-B16*, *shC002-B16*, and B16 cells (1×10^6) on the leg. Tumor size was measured on three orthogonal axes (*a*, *b*, and *c*) every 3–4 days, and tumor volumes were calculated as *abc*/2. The tumors were fixed in 10 % neutral formalin and embedded, and serial sections were histologically stained with H&E and were subjected to immunohistochemistry to visualize CD11b myeloid, F4/80 macrophage, and $CD8^+$ T cells. $CD8^+$ T cells or NK cells were depleted by injecting 100 μg/kg of anti-CD8 (clone 2.43.1) or anti-NK1.1 (clone PK136, BD Pharmingen, CA) antibodies, respectively, administered on days 14 and 21. Depletion was confirmed by flow cytometry analysis of peripheral blood using BD Pharmingen fluorescent-labeled anti-CD8α-FITC and anti-NK-PerCP antibodies [23].

Statistical analysis

One-way ANOVA and Dunnett's posttest were performed using GraphPad InStat version 3.05 to compare the average volumes of tumors in different experimental groups. Two-tailed Student's *t*-tests were performed to compare the means of the different treatment groups. $p < 0.05$ was accepted as significant.

Results

ShMaml1-B16 cells demonstrated greater cell differentiation and senescence

Stable clones of the *shMaml1-B16* cell line (shM138, shM140, shMmix) were established. Compared to the nontarget plasmid *shC002-B16*, the successful targeting of *Maml1*-promoted cell differentiation was demonstrated by increased melanin production. *ShMaml1-B16* cells exhibited a large, flat morphology indicative of senescence, which was confirmed by enhanced SA-β-gal staining (Fig. 1a). A protein analysis of the B16 cells demonstrated

the constitutive cleavage and high levels of expression of Notch 1 and Notch 4 but showed only low levels of expression of the Wnt signaling protein β-catenin, suggesting a dominant role for Notch signaling in B16 melanoma cells (we could not detect Hedgehog signaling protein, data not shown) (Fig. 1b). Total RNA was isolated from stable *shMaml1-B16*, *shC002-B16*, and parental B16 tumor cells, and RT-qPCR showed that the transcriptional repressors Hey1 and Hes1 abolished downstream Notch signaling (Fig. 1c). *ShMaml1-B16* cells proliferated less than *shC002-B16* or parental B16 tumor cells, but the difference in apoptotic rates among all cell lines was not significant in vitro (Fig. 1d).

Senescent shMaml1-B16 cells exhibited upregulated IFNβ and chemokine gene transcripts with increased STAT1 activity

Compared to *shC002-B16* or parent B16 tumor cells, *shMaml1-B16* cells showed greater expression of senescence-related cell cycle regulatory genes, including the cyclin-dependent kinase inhibitors $p16^{INK4A}$, $p21^{Cip1/Waf1}$, $p27^{Kip1}$, and $p57^{Kip2}$ (Fig. 2a). The expression levels of the *IFNβ*, *CCL2*, *CCL5*, and *CCL18* transcripts were also increased in *shMaml1-B16* cells relative to the *shC002-B16* or parent B16 tumor cells (Fig. 2b).

STATs and NF-κB have been reported to play essential roles in the synergistic transcriptional activation of multiple chemokines [23–25]. We analyzed the expression and activation of these signaling pathways in *shMaml1-B16*, *shC002-B16*, and parental B16 cells. Western blot analysis showed an increase in both the total and phosphorylated levels of STAT1 in the *shMaml1-B16* cells, but the phosphorylation of STAT3 and IκBα was inhibited (Fig. 2c). In the same cell line, inhibition of STAT1 with fludarabine blocked the expression of CCL2, CCL5, and IFNβ; however, inhibition of STAT3 using LLL12 or inhibition of IκBα kinase using BMS-345541 did not affect the expression of CCL2, CCL5, and IFNβ (Fig. 2d).

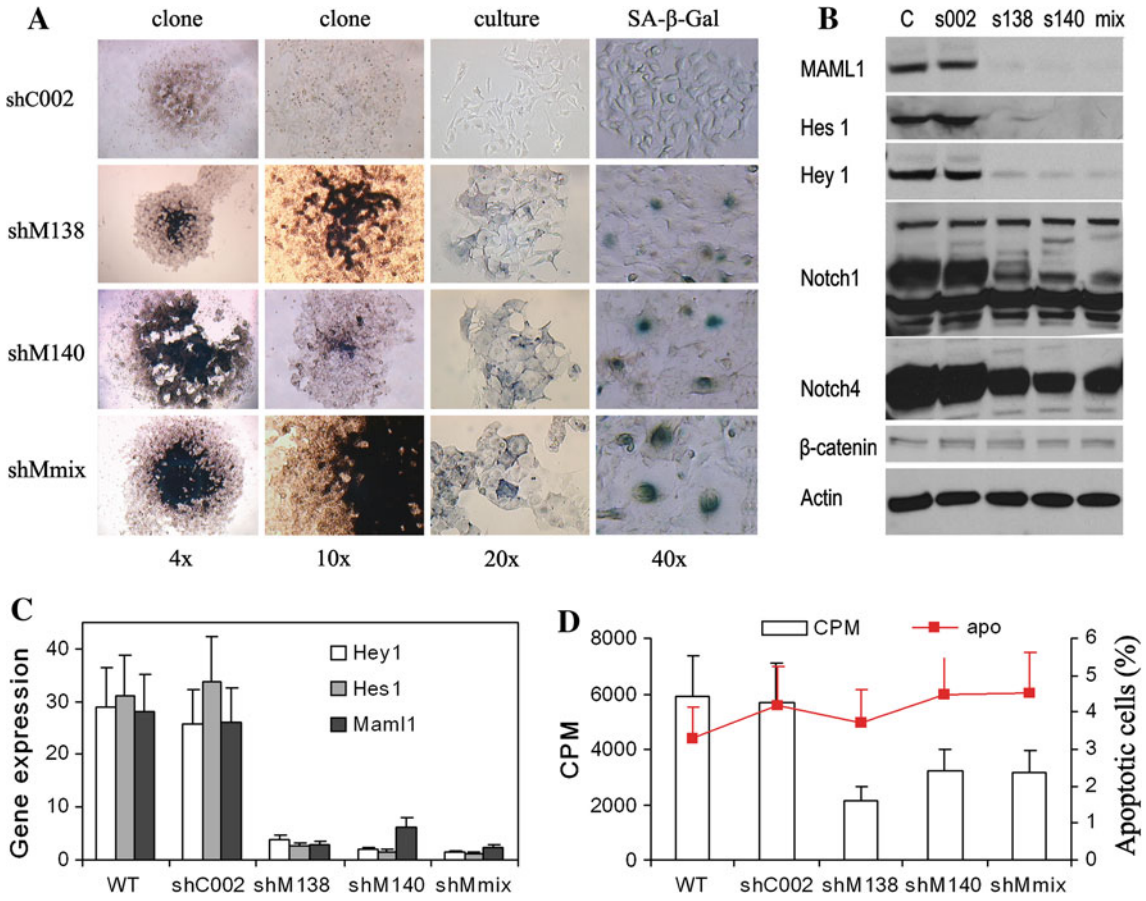

Fig. 1 Establishment and characterization of a stable *shMaml1-B16* cell line. **a** *ShMaml1-B16* cells exhibited more intracellular melanin production and SA-β-gal staining than control cells. **b** Western blot of Notch and Wnt signaling proteins in B16 cells. **c** Successful knockdown of the transcriptional repressors Hey1 and Hes1, as well as *Maml1*, in *shMaml1-B16* cells. **d** A lower proliferation rate but similar apoptosis rates are shown in *shMaml1-B16* cells relative to *shC002-B16* and parental WT B16 cells

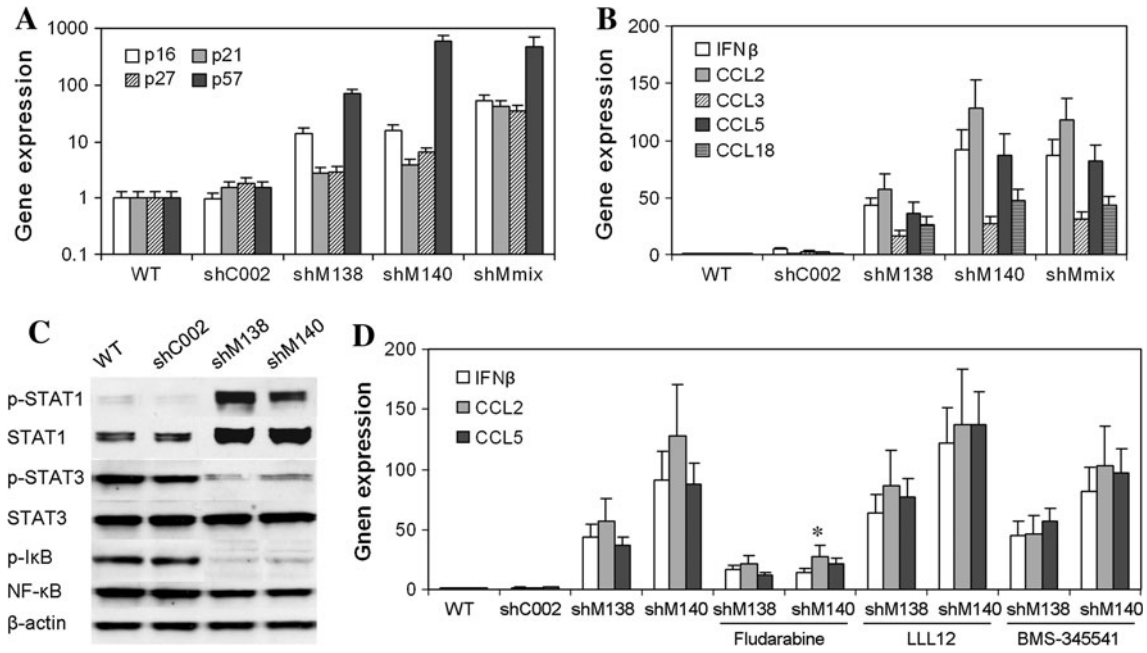

Fig. 2 Changes in cytokine and chemokine expression in senescent *shMaml1-B16* cells. **a** Upregulation of the cyclin-dependent kinase inhibitors $p16^{INK4A}$, $p21^{Cip1/Waf1}$, $p27^{Kip1}$, and $p57^{Kip2}$ in *shMaml1-B16* cells compared to *shC002-B16* or parent B16 tumor cells. **b** Upregulation of IFNβ, CCL2, CCL5, and CCL18 transcripts in *shMaml1-B16* cells. **c** Levels of total and phosphorylated STAT1 were increased in *shMaml1-B16* cells, but the phosphorylation of STAT3 and IκBα was inhibited. **d** Inhibition of STAT1 with fludarabine blocked the expression of CCL2, CCL5, and IFNβ in *shMaml1-B16* cells, $*p < 0.01$

Senescent shMaml1-B16 cells showed slower growth and increased immune cell infiltration in vivo

C57BL/6 mice were inoculated with *ShMaml1-B16*, *shC002-B16*, or parental B16 tumor cells (1×10^6). Tumor growth was observed, and the mean tumor volumes were calculated. The *ShMaml1-B16* tumors were smaller than both the *shC002-B16* and parental B16 tumors at day 18 ($p = 0.015$, $p = 0.013$) (Fig. 3a). RT-qPCR of tumor lysates showed a higher expression of *IFNγ*, *IFNβ*, *CCL2*, *CCL5*, *CXCL9*, *CXCL10*, and *CXCL11* in the *shMaml1-B16* tumors, thereby demonstrating that these cells are in an immunostimulatory microenvironment (Fig. 3b). Flow cytometry showed a higher frequency of $CD4^+$ T, $CD8^+$ T, and NK cells in the *shMaml1-B16* tumors compared to the frequency in the *shC002-B16* or parental B16 tumor cells (Fig. 3c). Depletion of NK ($p = 0.026$) and $CD8^+$ T ($p = 0.021$) cells in the *shMaml1-B16* tumor carrier mice led to a tumor growth rate that resembled the *shC002-B16* tumor growth rate. These data demonstrate that a knockdown of *Maml1* transcription and function contributes to slowed tumor growth not only by lowering the relative tumor cell proliferation rate but also through an increased infiltration of innate and adaptive immune cells (Fig. 3d). CD4 depletion ($p = 0.144$) did not change the growth rate of the *shMaml1-B16* tumors. Depletion of NK ($p = 0.175$) or $CD8^+$ T ($p = 0.217$) cells in the control *shC002-B16* tumor carriers did not significantly change the tumor growth rate.

Induction of cellular senescence in human melanoma cells transfected with shMaml1

Stable clones of the *shMaml1-M537* cell line (shM353, shM356) were established. Compared to the nontarget plasmid *shC002-M537*, the successful targeting of *Maml1*-promoted cell senescence was indicated by the large, flat morphology of the cells and enhanced SA-β-gal staining (Fig. 4a). Total RNA was isolated from stable *shMaml1-M537*, *shC002-M537*, and parental *M537* tumor cells, and RT-qPCR confirmed that the *Hey1/Hes1* and *Maml1* transcriptional repressors were knocked down (data not shown). The cyclin-dependent kinase inhibitors $p16^{INK4A}$, $p21^{Cip1/Waf1}$, and $p57^{Kip2}$ were upregulated compared to the *shC002-M537* or parent M537 tumor cells (Fig 4b, upper panel). Additionally, the expression of the *IFNβ*, *CCL2*, *CCL3*, *CCL5*, and *CXCL9* transcripts in the *shMaml1*-M537 cells was increased compared to the expression of these transcripts in the *shC002-M537* or parental M537 tumor cells (Fig 4b, lower panel). Finally, in a transwell system, the *shMaml1-M537* cells attracted more NK ($p < 0.05$) and $CD8^+$ T ($p < 0.01$) cells compared to the *shC002-M537* or parental M537 tumor cells (Fig 4c).

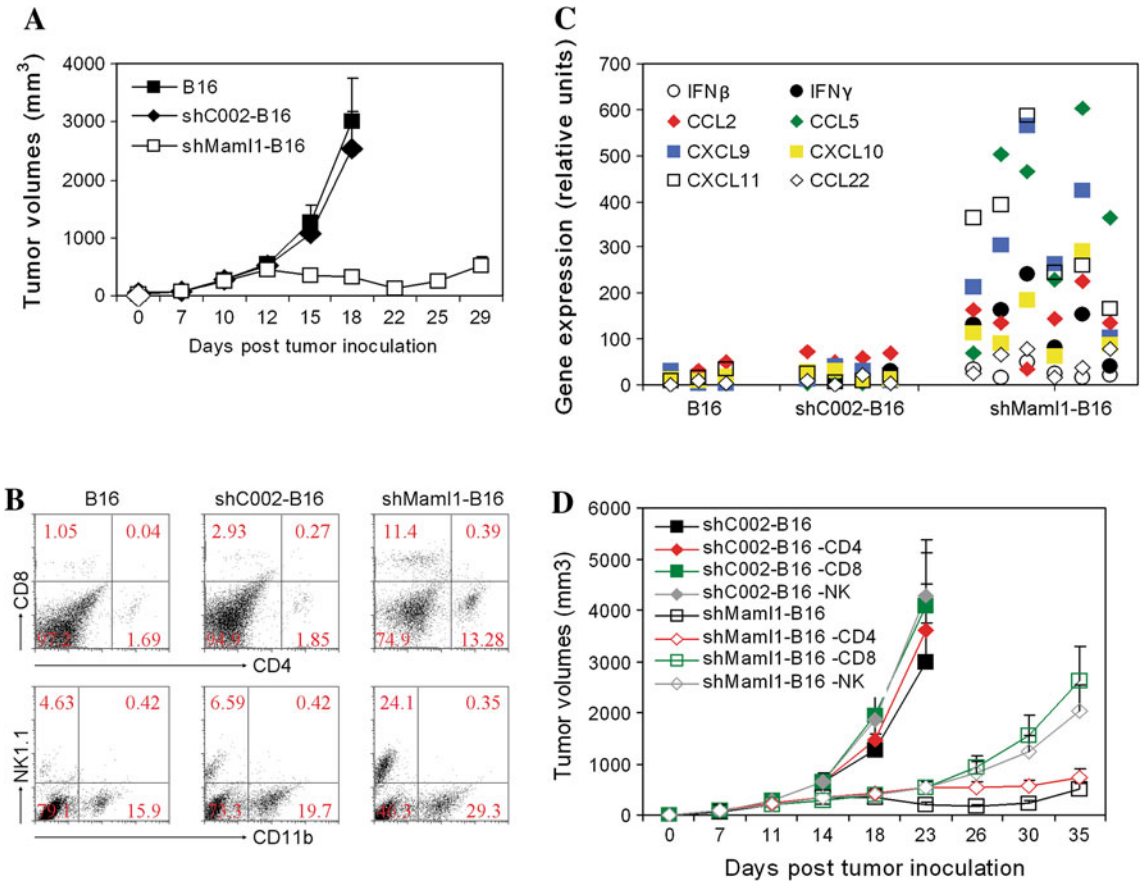

Fig. 3 Inhibition of senescent *shMaml1-B16* tumor growth and increased immune cell infiltration. **a** Growth curves of *shMaml1-B16*, *shC002-B16*, or parental B16 tumor cells in syngeneic C57BL/6 mice. **b** RT-qPCR of immune cytokine and chemokine expression in *shMaml1-B16* tumor lysates compared to *shC002-B16* or parental WT B16 tumor cells. **c** Flow cytometry of tumor-infiltrating cells in *shMaml1-B16* tumors. **d** Depletion of NK and $CD8^+$ T cells accelerated *shMaml1-B16* tumor growth

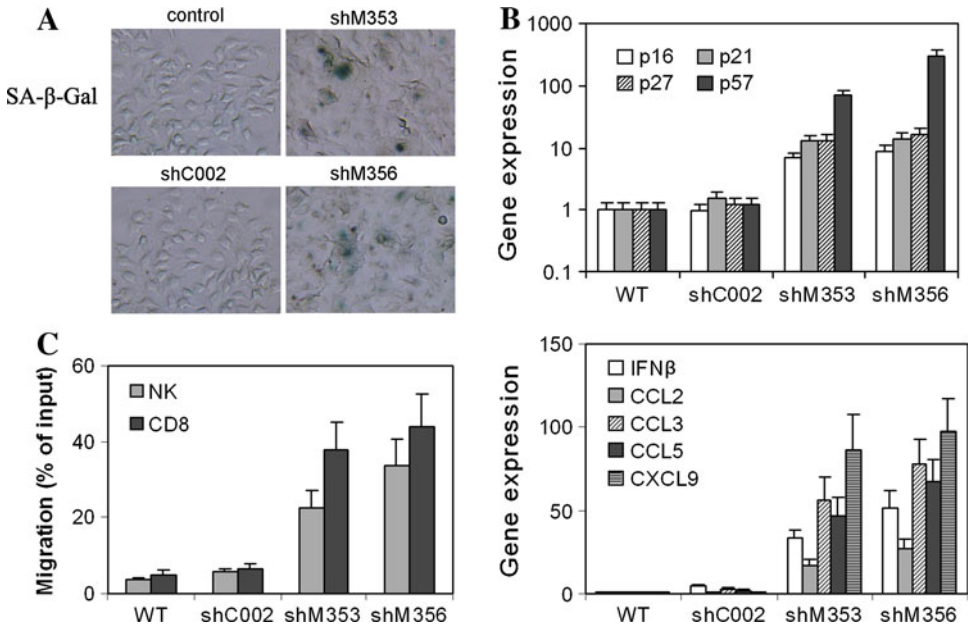

Fig. 4 Senescent *shMaml1-M537* cells expressed multiple cytokines and are more chemoattractive to NK and $CD8^+$ T cells. **a** *ShMaml1-M537* exhibited more SA-β-gal staining cells than control cells. **b** Upregulation of the cyclin-dependent kinase inhibitors $p16^{INK4A}$, $p21^{Cip1/Waf1}$, $p27^{Kip1}$, and $p57^{Kip2}$ in *shMaml1-M537* cells compared to *shC002-M537* or parent M537 tumor cells (*upper panel*). Upregulation of IFNβ, CCL2, CCL5, and CXCL9 transcripts in *shMaml1-M537* cells (*lower panel*). **c** Migration assay of NK and $CD8^+$ T cells in a transwell system that contains *shC002-M537*, *shC002-M537*, or parental M537 cells

Discussion

In this study, we show that a knockdown of Maml1 in melanoma cells results in tumor cell senescence and differentiation, leading to an upregulation of multiple immune cytokines and chemokines in the tumor microenvironment. This investigation further demonstrated that disrupting Maml1–Hes1-induced transcription repression improved immune surveillance and eventually contributed to the elimination of senescent tumor cells [23]. Wnt signaling results in the repression of $p21^{Cip1/Waf1}$, whereas Notch signaling represses $p27^{Kip1}$ and $p57^{Kip2}$ in part through its target gene *Hes1* [26, 27]. We knocked down Maml1, a coactivator known to participate in both Notch- and Wnt-activated *Hes1* transcription, in B16 melanoma cells. The knockdown effectively repressed the cyclin-dependent kinase inhibitors $p16^{INK4A}$, $p21^{Cip1/Waf1}$, $p27^{Kip1}$, and $p57^{Kip2}$, resulting in decreased cell proliferation and senescence [14, 17, 27]. Maml1 is emerging as a coactivator for many other pathways, but this report is the first to show that the inhibition of Maml1–Hes1 signaling induces cellular senescence and immune surveillance.

Maml1 was shown to cause the phosphorylation of IκBα and affect IκBα stability. Maml1 also acts as a coactivator of the NF-κB subunit p65 in NF-κB-dependent transcription. These findings indicate that Maml1 is a novel modulator of NF-κB signaling and has a role in the regulation of cell survival [28, 29]. The activation or suppression of *Notch1* and *Hes1* has been correlated with the phosphorylation and activation of STAT3, and targeting the STAT3/p63/Notch axis induces several types of tumor cell differentiation [30–32]. Additionally, interactions between activated STAT3 and constitutively active NF-κB have been studied in tumors by Yu's group, and STAT3 was shown to be a target for enhancing anti-tumor immunity [33–36]. Here, we show that targeting the Notch/Wnt coactivator Maml1 results in melanoma cell differentiation and senescence that not only inhibits the activation of both STAT3 and NF-κB but also stimulates the activity of STAT1. Consequently, the expression of immune cytokines and chemokines is significantly increased, resulting in increased NK and $CD8^+$ T cell infiltration and the establishment of an immunostimulatory microenvironment [36, 37].

Tumor cell differentiation has been associated with the activation of cellular senescence [38]. Treatments that induce senescence and tumor cell differentiation may need to be accompanied by chemotherapeutic drugs or radiation. Treatment-induced senescence was shown to be one of the key determinants of tumor response to therapy both in vitro and in vivo. Clinical and preclinical studies have shown that the expression of different biological classes of senescence-associated genes in tumor cells has significant prognostic implications [39–41]. Although senescent cells do not proliferate, they remain metabolically active and secrete proteins with either tumor-suppressing or tumor-promoting activities [42, 43]. A role has been reported for the innate immune system in eliminating senescent cells from tumors upon p53 reexpression, and $CD4^+$ T cells have been shown to mediate anti-tumor effects through Myc-induced cellular senescence [44, 45]. We have shown that mouse *shMaml1-B16* cells and human *shMaml1-M537* cells undergoing senescence expressed multiple senescence-associated immune cytokines and chemokines, both in culture and in tumor microenvironments. Consequently, more NK and $CD8^+$ T cell infiltrations occurred, demonstrating that the disruption of Maml1- and Notch-induced transcription repression may be a possible strategy for cancer treatment. Maml1 may participate in the Notch and Wnt signaling pathways during normal tissue development and cell differentiation; the knockdown of Maml1 blocked the transcriptional repression of *Hes1* and affected the activation of STAT1, STAT3, and NF-κB. This specific knockdown of Maml1 in tumor cells has tremendous therapeutic potential; therefore, further studies of the involvement of Maml1 in the Notch and Wnt pathways are necessary.

Acknowledgments This work was supported by the Province of Guangdong Science Grant (10251051501000008).

Conflict of interest The authors declare that they have no conflict of interest.

References

1. Takebe N, Harris PJ, Warren RQ, Ivy SP (2011) Targeting cancer stem cells by inhibiting Wnt, Notch, and Hedgehog pathways. Nat Rev Clin Oncol 8:97–106
2. Zhou BB, Zhang H, Damelin M, Geles KG, Grindley JC, Dirks PB (2009) Tumour-initiating cells: challenges and opportunities for anticancer drug discovery. Nat Rev Drug Discov 8:806–823
3. Crea F, Duhagon MA, Farrar WL, Danesi R (2011) Pharmacogenomics and cancer stem cells: a changing landscape? Trends Pharmacol Sci 32:487–494
4. Radtke F, Raj K (2003) The role of Notch in tumorigenesis: oncogene or tumour suppressor? Nat Rev Cancer 3:756–767
5. Hansson EM, Lendahl U, Chapman G (2004) Notch signaling in development and disease. Semin Cancer Biol 14:320–328
6. Nickoloff BJ, Osborne BA, Miele L (2003) Notch signaling as a therapeutic target in cancer: a new approach to the development of cell fate modifying agents. Oncogene 22:6598–6608
7. Kang S, Yang C, Luo R (2008) Induction of CCL2 by siMAML1 through upregulation of TweakR in melanoma cells. Biochem Biophys Res Commun 372:629–633
8. Kopan R, Ilagan MX (2009) The canonical Notch signaling pathway: unfolding the activation mechanism. Cell 137:216–233
9. Alves-Guerra MC, Ronchini C, Capobianco AJ (2007) Mastermind-like 1 Is a specific coactivator of beta-catenin transcription activation and is essential for colon carcinoma cell survival. Cancer Res 67:8690–8698

10. Shimizu T, Kagawa T, Inoue T, Nonaka A, Takada S, Aburatani H, Taga T (2008) Stabilized beta-catenin functions through TCF/LEF proteins and the Notch/RBP-Jkappa complex to promote proliferation and suppress differentiation of neural precursor cells. Mol Cell Biol 28:7427–7441
11. Ingram WJ, McCue KI, Tran TH, Hallahan AR, Wainwright BJ (2008) Sonic Hedgehog regulates Hes1 through a novel mechanism that is independent of canonical Notch pathway signalling. Oncogene 27:1489–1500
12. Wall DS, Mears AJ, McNeill B, Mazerolle C, Thurig S, Wang Y, Kageyama R, Wallace VA (2009) Progenitor cell proliferation in the retina is dependent on Notch-independent Sonic hedgehog/Hes1 activity. J Cell Biol 184:101–112
13. Hatton BA, Villavicencio EH, Pritchard J, LeBlanc M, Hansen S, Ulrich M, Ditzler S, Pullar B, Stroud MR, Olson JM (2010) Notch signaling is not essential in sonic hedgehog-activated medulloblastoma. Oncogene 29:3865–3872
14. Sang L, Roberts JM, Coller HA (2010) Hijacking HES1: how tumors co-opt the anti-differentiation strategies of quiescent cells. Trends Mol Med 16:17–26
15. Schreck KC, Taylor P, Marchionni L, Gopalakrishnan V, Bar EE, Gaiano N, Eberhart CG (2010) The Notch target Hes1 directly modulates Gli1 expression and Hedgehog signaling: a potential mechanism of therapeutic resistance. Clin Cancer Res 16:6060–6070
16. Sang L, Coller HA (2009) Fear of commitment: Hes1 protects quiescent fibroblasts from irreversible cellular fates. Cell Cycle 8:2161–2167
17. Sang L, Coller HA, Roberts JM (2008) Control of the reversibility of cellular quiescence by the transcriptional repressor HES1. Science 321:1095–1100
18. Wu L, Kobayashi K, Sun T, Gao P, Liu J, Nakamura M, Weisberg E, Mukhopadhyay NK, Griffin JD (2004) Cloning and functional characterization of the murine mastermind-like 1 (Maml1) gene. Gene 328:153–165
19. Jin B, Shen H, Lin S, Li JL, Chen Z, Griffin JD, Wu L (2010) The mastermind-like 1 (MAML1) co-activator regulates constitutive NF-kappaB signaling and cell survival. J Biol Chem 285:14356–14365
20. Hanahan D, Weinberg RA (2000) The hallmarks of cancer. Cell 100:57–70
21. Moellering RE, Cornejo M, Davis TN, Del Bianco C, Aster JC, Blacklow SC, Kung AL, Gilliland DG, Verdine GL, Bradner JE (2009) Direct inhibition of the NOTCH transcription factor complex. Nature 462:182–188
22. Bartlett DW, Davis ME (2006) Insights into the kinetics of siRNA-mediated gene silencing from live-cell and live-animal bioluminescent imaging. Nucleic Acids Res 34:322–333
23. Kang S, Xie J, Ma S, Liao W, Zhang J, Luo R (2010) Targeted knock down of CCL22 and CCL17 by siRNA during DC differentiation and maturation affects the recruitment of T subsets. Immunobiology 215:153–162
24. Hiroi M, Ohmori Y (2003) Constitutive nuclear factor kappaB activity is required to elicit interferon-gamma-induced expression of chemokine CXC ligand 9 (CXCL9) and CXCL10 in human tumour cell lines. Biochem J 376:393–402
25. Biswas SK, Gangi L, Paul S, Schioppa T, Saccani A, Sironi M, Bottazzi B, Doni A, Vincenzo B, Pasqualini F, Vago L, Nebuloni M, Mantovani A, Sica A (2006) A distinct and unique transcriptional program expressed by tumor-associated macrophages (defective NF-kappaB and enhanced IRF-3/STAT1 activation). Blood 107:2112–2122
26. Riccio O, van Gijn ME, Bezdek AC, Pellegrinet L, van Es JH, Zimber-Strobl U, Strobl LJ, Honjo T, Clevers H, Radtke F (2008) Loss of intestinal crypt progenitor cells owing to inactivation of both Notch1 and Notch2 is accompanied by derepression of CDK inhibitors p27Kip1 and p57Kip2. EMBO Rep 9:377–383
27. Kavanagh E, Joseph B (2011) The hallmarks of CDKN1C (p57, KIP2) in cancer. Biochim Biophys Acta 1816:50–56
28. Jin B, Shen H, Lin S, Li JL, Chen Z, Griffin JD, Wu L (2010) The mastermind-like 1 (MAML1) co-activator regulates constitutive NF-kappaB signaling and cell survival. J Biol Chem 285:14356–14365
29. Cao Q, Kaur C, Wu CY, Lu J, Ling EA (2011) Nuclear factor-kappa beta regulates Notch signaling in production of proinflammatory cytokines and nitric oxide in murine BV-2 microglial cells. Neuroscience 192:140–154
30. Bhoopathi P, Chetty C, Dontula R, Gujrati M, Dinh DH, Rao JS, Lakka SS (2011) SPARC stimulates neuronal differentiation of medulloblastoma cells via the Notch1/STAT3 pathway. Cancer Res 71:4908–4919
31. Lee JH, Suk J, Park J, Kim SB, Kwak SS, Kim JW, Lee CH, Byun B, Ahn JK, Joe CO (2009) Notch signal activates hypoxia pathway through HES1-dependent SRC/signal transducers and activators of transcription 3 pathway. Mol Cancer Res 7:1663–1671
32. Ma J, Meng Y, Kwiatkowski DJ, Chen X, Peng H, Sun Q, Zha X, Wang F, Wang Y, Jing Y, Zhang S, Chen R, Wang L, Wu E, Cai G, Malinowska-Kolodziej I, Liao Q, Liu Y, Zhao Y, Xu K, Dai J, Han J, Wu L, Zhao RC, Shen H, Zhang H (2010) Mammalian target of rapamycin regulates murine and human cell differentiation through STAT3/p63/Jagged/Notch cascade. J Clin Invest 120:103–114
33. Lee H, Deng J, Xin H, Liu Y, Pardoll D, Yu H (2011) A requirement of STAT3 DNA binding precludes Th-1 immunostimulatory gene expression by NF-kappaB in tumors. Cancer Res 71:3772–3780
34. Lee H, Herrmann A, Deng JH, Kujawski M, Niu G, Li Z, Forman S, Jove R, Pardoll DM, Yu H (2009) Persistently activated Stat3 maintains constitutive NF-kappaB activity in tumors. Cancer Cell 15:283–293
35. Lee H, Pal SK, Reckamp K, Figlin RA, Yu H (2011) STAT3: a target to enhance antitumor immune response. Curr Top Microbiol Immunol 344:41–59
36. Yu H, Pardoll D, Jove R (2009) STATs in cancer inflammation and immunity: a leading role for STAT3. Nat Rev Cancer 9:798–809
37. Regis G, Pensa S, Boselli D, Novelli F, Poli V (2008) Ups and downs: the STAT1:STAT3 seesaw of Interferon and gp130 receptor signalling. Semin Cell Dev Biol 19:351–359
38. Pinho AV, Rooman I, Reichert M, De Medts N, Bouwens L, Rustgi AK, Real FX (2011) Adult pancreatic acinar cells dedifferentiate to an embryonic progenitor phenotype with concomitant activation of a senescence programme that is present in chronic pancreatitis. Gut 60:958–966
39. Lleonart ME, Artero-Castro A, Kondoh H (2009) Senescence induction; a possible cancer therapy. Mol Cancer 8:3
40. Roninson IB (2003) Tumor cell senescence in cancer treatment. Cancer Res 63:2705–2715
41. Schmitt CA (2007) Cellular senescence and cancer treatment. Biochim Biophys Acta 1775:5–20
42. Kahlem P, Dorken B, Schmitt CA (2004) Cellular senescence in cancer treatment: friend or foe? J Clin Invest 113:169–174
43. Freund A, Orjalo AV, Desprez PY, Campisi J (2010) Inflammatory networks during cellular senescence: causes and consequences. Trends Mol Med 16:238–246
44. Xue W, Zender L, Miething C, Dickins RA, Hernando E, Krizhanovsky V, Cordon-Cardo C, Lowe SW (2007) Senescence and tumour clearance is triggered by p53 restoration in murine liver carcinomas. Nature 445:656–660
45. Rakhra K, Bachireddy P, Zabuawala T, Zeiser R, Xu L, Kopelman A, Fan AC, Yang Q, Braunstein L, Crosby E, Ryeom S, Felsher DW (2010) CD4(+) T cells contribute to the remodeling of the microenvironment required for sustained tumor regression upon oncogene inactivation. Cancer Cell 18:485–498